Dispersion engineering of superconducting waveguides for multi-pixel integration of single-photon detectors ⓕ

🅓 Ali W. Elshaari, 🅓 Adrian Iovan, 🅓 Samuel Gyger, 🅓 Iman Esmaeil Zadeh, Julien Zichi, 🅓 Lily Yang, 🅓 Stephan Steinhauer, and 🅓 Val Zwiller

COLLECTIONS

ⓕ   This paper was selected as Featured

View Online   Export Citation   CrossMark

Dispersion engineering of superconducting waveguides for multi-pixel integration of single-photon detectors Ⓕ

View Online   Export Citation   CrossMark

Ali W. Elshaari,[1,a] ⓘ Adrian Iovan,[1] ⓘ Samuel Gyger,[1] ⓘ Iman Esmaeil Zadeh,[2] ⓘ Julien Zichi,[1] Lily Yang,[1] ⓘ
Stephan Steinhauer,[1] ⓘ and Val Zwiller[1] ⓘ

AFFILIATIONS

[1] Department of Applied Physics, Royal Institute of Technology, Albanova University Centre, Roslagstullsbacken 21,
106 91 Stockholm, Sweden

[2] Optics Research Group, ImPhys Department, Faculty of Applied Sciences, TU Delft, Lorentzweg 1,
2628 CJ Delft, The Netherlands

[a] Author to whom correspondence should be addressed: elshaari@kth.se

ABSTRACT

We use dispersion engineering to control the signal propagation speed in the feed lines of superconducting single-photon detectors. Using this technique, we demonstrate time-division-multiplexing of two-pixel detectors connected with a slow-RF transmission line, all realized using planar geometry requiring a single lithographic step. Through studying the arrival time of detection events in each pixel vs the fabricated slow-RF coplanar waveguide length, we extract a delay of 1.7 ps per 1 μm of propagation, corresponding to detection signal speeds of ~0.0019c. Our results open an important avenue to explore the rich ideas of dispersion engineering and metamaterials for superconducting detector applications.

Superconducting nanowire single-photon detectors (SNSPDs) with their close-to-unity detection efficiencies,[1] wide operating-wavelength range,[1,2] sub-3-ps timing resolution,[3] and versatile integration with different photonic platforms[4–6] are central resources for quantum information technologies.[7,8] Extensive work has been done to optimize SNSPDs' operation and understanding the physical limits of their performance, additionally photon-number resolution was demonstrated through parallel connections of SNSPDs,[10] and by engineering the detector transmission line for impedance matching.[11,12] More recently, an important goal is to realize large-scale systems making use of their attractive detection characteristics[13] while achieving high reproducibility and control over their performance.[6] In order to integrate multiple detectors on a single chip, a straightforward approach would be to include independent RF feed lines for each individual detector. This might be viable for systems with a small number of detectors[14] but becomes increasingly challenging when aiming for large-scale

integration. The thermal budget in such circumstances becomes very important,[15] both the passive and active thermal loads for the detectors set a practical limit for the number of detectors. As an example, the total thermal load for 50 superconducting qubit systems is close to 150 mW at the 4 K stage.[15] Although superconducting detectors are less involved than operating a qubit in terms of electrical connections and readout, similar heat load challenges would limit realizing large-scale systems. Moreover, cost becomes important for implementing electronic readout and biasing circuits for every single channel. Additionally, data processing becomes nontrivial when aiming for 1000s of detectors operating at GHz speeds. More sophisticated approaches for multi-pixel integration include frequency-,[16] amplitude-,[17,18] and time-multiplexing;[19–22] each technique has its own advantages and drawbacks. Frequency multiplexing requires precise tone generation to address individual SNSPDs, coupled with the stringent requirement to fine-tune the resonance circuits of individual detectors (or the driving frequency). This places practical

limits on the complexity and number of detectors that can be addressed, in addition to modulation of the detection efficiency with the driving signal. Amplitude multiplexing, on the other hand, provides a simpler alternative but is more susceptible to noise and errors, which can limit the number of identifiable logic levels; such a limitation is a common feature to amplitude modulation techniques.[23] Time multiplexing has an advantage in terms of operation simplicity, but two main challenges must be addressed as follows: (1) an individual detector jitter needs to be minimized, setting a lower limit on time-bin size, and (2) the high on-chip RF propagation velocity places practical limits on the devices' dimensions to achieve the needed delay for time multiplexing.[20] Recent demonstrations[19,21,22] show the possibility to reduce the group velocity of detection pulses on a chip. A multi-layer integration approach can set limits on the device design and integration, especially co-integration with planar photonic integrated circuits. Moreover, further reduction in the detection pulse speed in planar geometries is important for dense integration of multiple pixels. Here, we apply the powerful technique of waveguide dispersion engineering, commonly used for dielectric photonic circuits,[24] to superconducting transmission lines.[25] By operating in the slow-RF regime, we can address two detectors with a single transmission line, all using planar circuit geometry requiring only one lithographic step.

Figures 1(a) and 1(b) show a circuit diagram and a schematic of the coplanar transmission line connecting multiple pixels on the same chip. The waveguide consists of a distributed kinetic inductance of the superconducting wire capacitively coupled to ground. The velocity of the electromagnetic wave in the transmission line is inversely proportional to $\sqrt{LC}$, where C and L are the capacitance and inductance per unit length.[26] C can be designed using a coplanar circuit technology to control the speed of propagation. By engineering the capacitance value and its periodicity, a bandgap of forbidden frequencies can be introduced in the ω–k dispersion relation. Operating near the band edge yields vanishingly small group velocities, approaching zero at the band edge accompanied by a sharp increase in the reflected signal. The transmission line is designed and tested numerically through the method of moments, using the commercial 3D microwave simulation tool Sonnet.[27] The main transmission line is a 1 μm wide NbTiN wire, with a kinetic inductance of 40 pH/sq.[28] Superconducting wires with the same width extend on both sides of the main transmission line, each having a length of 1 mm. The side wires repeat every 13 μm; together with the ground plane, they form an interdigitated capacitor with a 1 μm gap. The simulated transmission line has six unit cells between the input and output ports. The width of the simulation region is 2 mm around the interdigitated capacitor, while the height is 2 mm including the silicon wafer thickness of 500 μm and an air layer. Figure 1(c) shows the scattering matrix parameters $S11$ and $S12$. The transmission shows a clear low-frequency pass by design (blue shaded), covering the area of interest of the SNSPD operation. The amplifier bandwidth of the driving circuit in the experimental setup is 1.2 GHz, and the device shows an almost flat low group velocity regime below this limit. Close to 5 GHz, our simulations show that the group delay of the RF signal increases drastically, as shown in Fig. 1(d). Although the detection signal can be significantly slowed in that regime, it also suffers from high group velocity dispersion and low transmission; thus, by design, the transmission-line resonance is placed beyond the amplifier bandwidth.
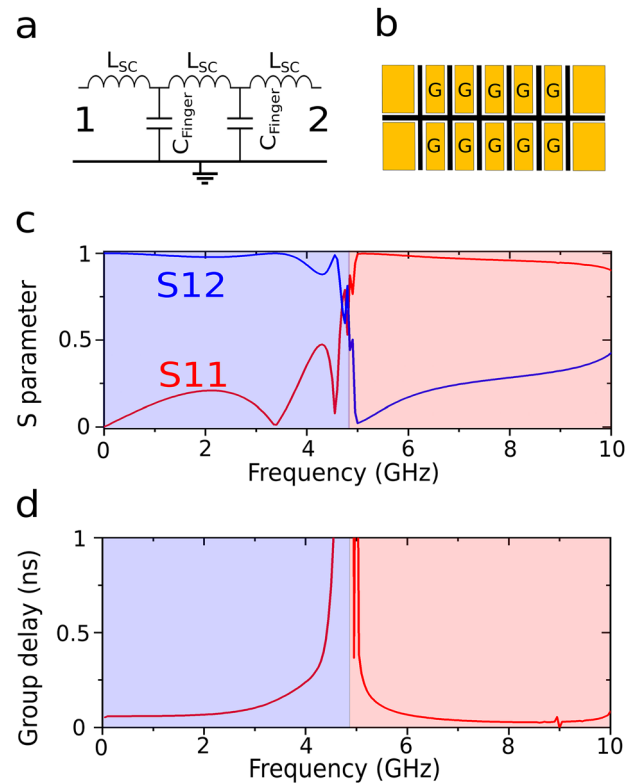

FIG. 1. (a) Circuit diagram of the transmission line. (b) Schematic of a capacitively coupled transmission line to ground, shown in yellow. The transmission line connects superconducting detectors in series. (c) Scattering parameters, $S11$ (red) and $S12$ (blue), between port 1 and port 2 in the simulated devices. The bandpass region is blue shaded, while the rejection band higher than the band edge is red-shaded. (d) Simulated group delay as a function of propagation frequency.

The circuits were fabricated based on the simulation design parameters. The fabrication involves sputtering 9 nm NbTiN films on a silicon wafer with a 180 nm thermal oxide superficial layer.[5,29] The circuits were patterned using diluted electron-beam resist ma-N 2403:mrT 1090 (1:1) and a 50 keV Raith e-beam lithography system. The pattern was transferred to the superconducting film by CF4-based reactive ion etching. A single pixel is shown in Fig. 2(a), consisting of a 100 nm constriction in the superconducting wire, thus limiting detection events to this area. Two pixels were connected with a transmission line consisting of N side capacitors, as shown in Fig. 2(b). A closer look at the capacitively coupled transmission line is shown in Fig. 2(c), with dimensions chosen to directly match the simulated structure. The experimental setup for testing the devices is shown schematically in Fig. 2(d). The sample is illuminated with a 780 nm 3-ps laser, with an 80 MHz repetition rate. The SNSPDs are cooled to a temperature of 2.5 K in a closed-cycle cryostat, considerably lower than their critical temperature. The critical temperature of the films is 10 K.[5,30] 2.5 K operation is required; higher temperatures reduce the detection efficiency especially for IR photons,[30] in addition to the overall lower critical current, which reduces the detection timing-resolution.[30] A room temperature bias-T
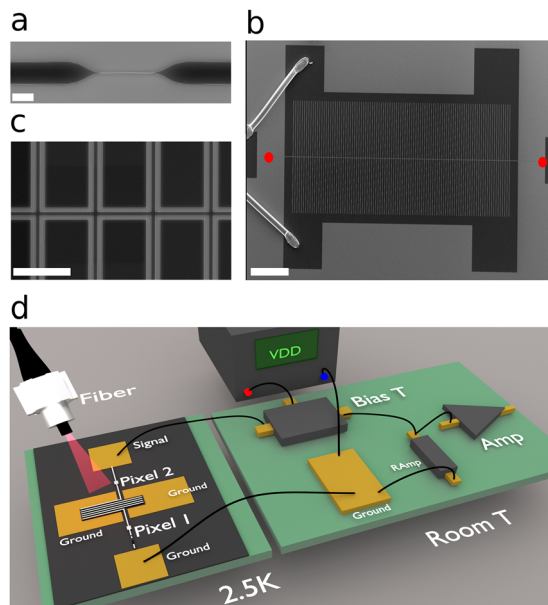
FIG. 2. (a) Scanning electron microscope image of a single 100 nm wide pixel, scale bar 1 μm. (b) Complete device with a slow-RF transmission line connecting two pixels highlighted by a red dot, scale bar 250 μm. In the shown device, the side capacitor length is reduced to easily visualize the complete circuit with the contacts. (c) Magnified view of the slow-RF coplanar transmission line, scale bar 13 μm. (d) Schematic of the experimental setup.

and an amplifier with a bandwidth of 1.2 GHz are used for current biasing of the detector and amplification of the detection pulses, respectively.

Several devices with different numbers of side capacitors were fabricated. A direct measurement of the group velocity of the transmission lines as a function of frequency is hard to measure experimentally as it requires a low temperature measurement of the frequency response of the transmission line, coupled with a frequency domain analysis of the detection pulse; the supplementary material provides numerical simulations of the transmission line. However, experimentally, we can investigate the effect of an increase in the length of the slow-RF transmission line on the arrival time of detection events from the two pixels, while keeping the physical distance between the two pixels fixed. Figure 3(a) shows the *IV* characteristic of a 60 side capacitor device. This two-pixel detector has a critical current of 13 μA, with signature of internal efficiency saturation under illumination from the laser. All the devices were biased at 90% of their critical currents. The detection pulses were correlated with an 80 MHz sync signal from the laser to build a histogram of the arrival time of detection events in each pixel. A single-side readout scheme was employed, with pixel 1 connected to the signal terminal, while pixel 2 and the interdigitated capacitor were connected to ground. The correlation measurements were recorded with a fast digital oscilloscope (Lecroy WaveRunner 640Zi, with 4 GHz bandwidth). Figure 3(b) shows four histograms for devices with 0, 30, 60, and 80 side capacitors. All the traces are plotted in reference to the arrival time of detection events in pixel 1. We clearly see an increase in the arrival time of detection events from pixel 2 as the number
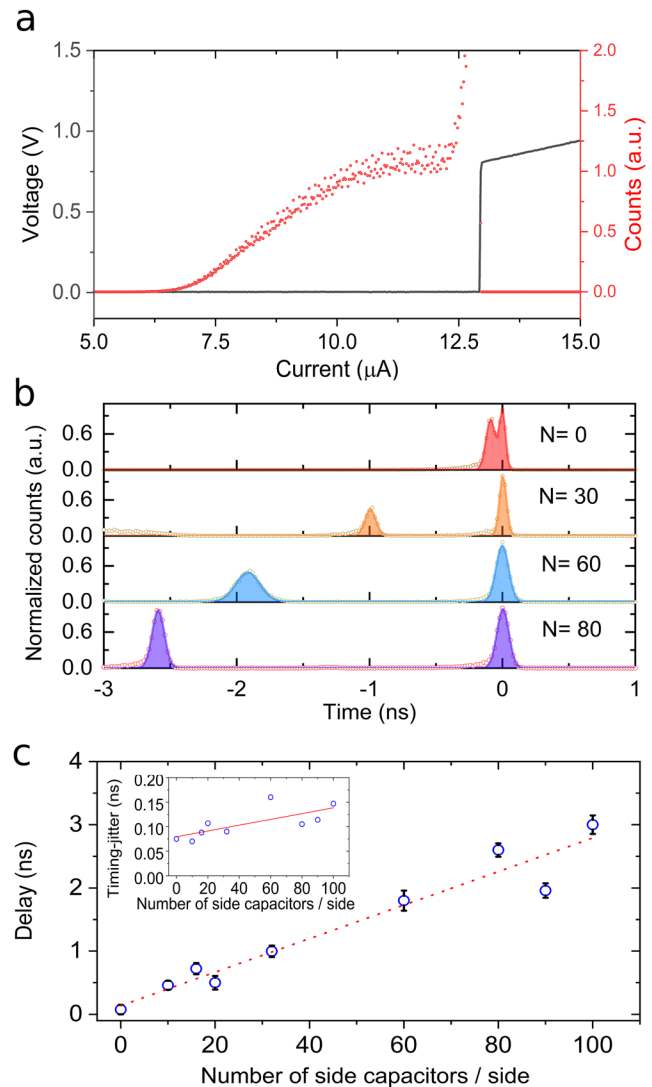

FIG. 3. (a) *IV* characteristic and detection counts for a 60 side capacitor device under illumination with 3-ps laser pulses at a wavelength of 780 nm. (b) Detection pulse arrival time of pixels 1 and 2 for devices with $N = 0$, 30, 60, and 80 side capacitors. The data are plotted with pixel 1 placed at zero delay as a reference. (c) Extracted delay for devices with different numbers of side capacitors on each side, linearly fitted to a straight line. The slope of the linear fit is 0.26 ± 0.03 ns per 10 side capacitors. The error bars present the timing jitter of the arrival time of the detection pulse. The inset shows the timing jitter of detection events for each device.

of side capacitors is increased. We extracted the measured temporal delay between the two pixels vs number of side capacitors, as shown in Fig. 3(c), with a linear fit of the data. The linear fit provides two parameters: an intercept that accounts for a fixed delay between the pixels for all the devices due to the device geometry, and a slope that describes the delay change with the number of side capacitors. The experimentally measured group delay between the two pixels is extracted from the slope of the fit to be 0.26 ± 0.03 ns per 10 side capacitors. The maximum measured delay in the 100 side capacitor

device corresponds to a group velocity of 0.19% of the speed of light in vacuum (1.7 ps delay per 1 μm of propagation), which is an order of magnitude smaller than the reported group velocities in single and multi-layered structures.[19,21]

The device is operated in a low group velocity dispersion regime, which can reduce the timing resolution due to detection pulse distortion. To quantify this effect, we extracted the timing jitter of the detection pulse vs the number of side capacitors, as shown in the inset of Fig. 3(c). To minimize the measurement error, 25 000 events were recorded. The linear fit intercept describes the inherent timing jitter in the system for all two-pixel devices. We focus on the slope that accounts for the rate at which the jitter changes with an increase in the number of side capacitors. The FWHM of the detection-pulse arrival-time histogram increases by 5.9 ± 2 ps per 10 side capacitors. An important figure of merit for time multiplexing superconducting single-photon detectors is the ratio of the delay between pixels in a time-domain to the FWHM of each time-bin. This sets a limit on the number of pixels multiplexed for a given delay. To provide a lower limit for the performance, the 100 side capacitor device showed the highest FWHM timing jitter of 147 ps (2.355σ). The demonstrated delay between pixel 1 and pixel 2 for the same device is 3 ns, 48 times larger than the timing-jitter σ. It is worth mentioning that the jitter can be further reduced using cryogenic amplifiers, boosting the figure of merit even further. This will also allow for reducing the footprint of the device since only a few periods of the side capacitors are needed to distinguish between detection events on the same transmission line.

Following the last point on the footprint of the devices, we investigated the effect of reducing the length of the side capacitor on the achieved delay. Figure 4(a) shows IV characteristic of two devices fabricated on the same chip. Each device consists of two pixels connected with a transmission line consisting of 100 capacitors on each side, but with two different side capacitor lengths, 600 μm and 1000 μm, respectively. The two devices have critical currents of 11.9 μA and 10.3 μA and are biased at 90% of their critical currents. Figure 4(b) shows the recorded detection event histogram of the two devices, using the same experimental configurations described earlier. The 1000 μm device shows only a 20% increase in the experimentally measured delay compared to the 600 μm device, despite the overall increase of 66% in the area between the two. To provide more insight into the behavior, both structures were simulated in Sonnet.[27] The simulation results of the ratio between group delays of different frequencies for the two devices are shown in Fig. 4(c). We see an increase of 20% in the group delay within the amplifier of 3 dB bandwidth, closely matching the experimental results. The increase in the shunt capacitance to ground by extending the length of the side wires moves the resonance frequency of the transmission line to lower frequencies. This results in an increase in the group delay ratio between the two devices as we approach the 1000 μm device band edge. Optimally, the device is designed to operate in the flat regime of the dispersion relation, far from the resonance frequency of the transmission line.

Figure 5 shows an envisioned application for the slow-RF superconducting transmission line. The device computes the Fourier transform of light signals on a chip; photons propagating in the waveguide from the forward and backward directions interfere at the center of the device; then, the standing wave pattern can be
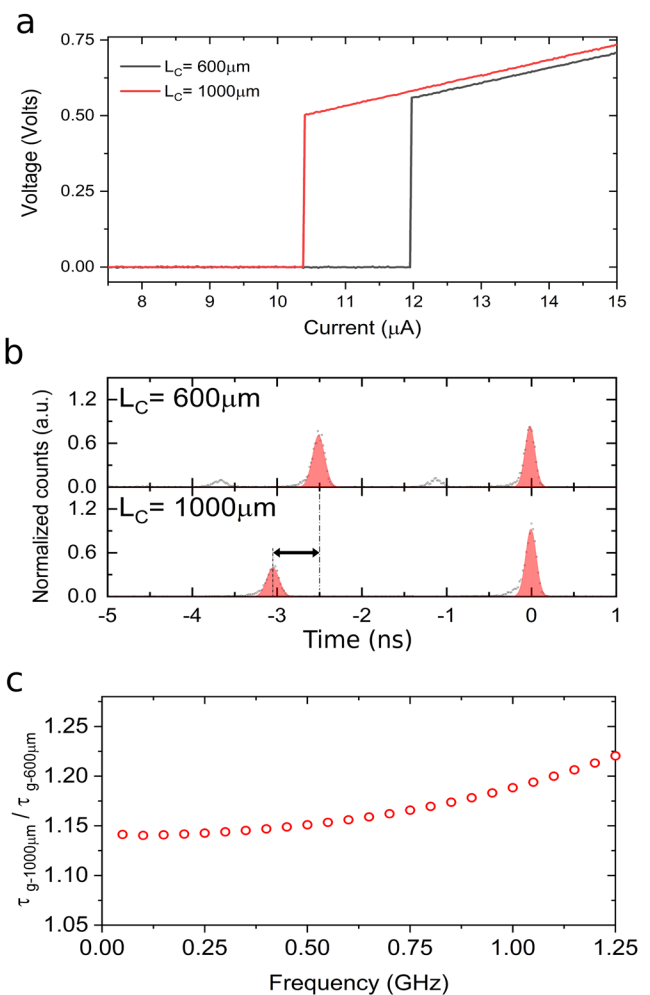

FIG. 4. (a) IV characteristic of two-pixel detectors having side capacitor lengths of 600 μm and 1000 μm. (b) Histogram of the detection events of the two devices, both referenced to detection events in pixel 1. (c) 3D microwave simulation of the ratio between group delays at different frequencies of the two devices.

sampled at the single-photon level using SNSPDs. The detector is classified as a stationary-wave integrated Fourier transform spectrometer (SWIFT).[31,32] In order to reconstruct the spectrum of the input signal, the Nyquist–Shannon criteria must be satisfied. This requires several numbers of independently operated detectors on the same chip, each with its own readout. We envision using the engineering of the superconducting single-photon detectors' transmission line to enable time-division-multiplexing of single-photon detectors on the same transmission line, thus using a single biasing and readout circuit for the multiple detectors. Moreover, the same technique can be used to demonstrate 2D imaging using SNSPD arrays connected through a single coaxial line.[21] The frame count rate for such devices is typically limited by the kinetic inductance of the detector;[21] thus, reducing the device dimensions would enable higher count rates.[33]
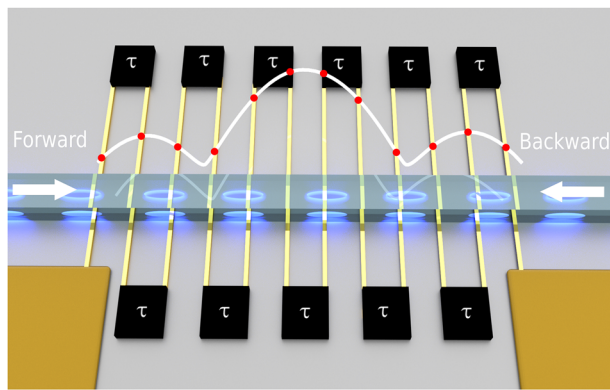
FIG. 5. Schematic of a SWIFT detector. Each pixel samples the standing wave pattern of the light signal interfering with itself in an interferometer. The device uses a single transmission line for readout, and pixels are multiplexed in a time-domain.

In summary, we employed the concepts of slow-light to superconducting transmission lines for time-division-multiplexing of SNSPDs. The slow-RF transmission line delivers a large on-chip delay of 1.7 ps per 1 μm of propagation. The demonstrated devices provide an excellent figure of merit for time-division-multiplexing. Although the physical distance between pixels can be reduced due to the smaller group velocity, the presented devices have a drawback of an overall larger area compared to other multiplexing approaches.[19,21,22] We believe that this is not a fundamental limit, and dispersion engineering can also be used to complement previous demonstrations, adding another level of control over the waveguide dispersion. Moreover, this work focused on the capacitive aspect of the periodic load of the transmission line, but the inductive part is as important to modify the overall line impedance for excellent matching to coaxial lines.[11,12] Our results open a wide range of possibilities to apply the already established field of dispersion engineering for a complex superconducting detector circuitry, which is critical for large-scale quantum photonic applications. In addition to the potential usage for on-chip feedback-control and synchronization of detection events on a chip,[8] we envision more advanced applications for matching photonic and microwave velocities in traveling structures[34] and metamaterial-based transmission lines for size reduction and bandwidth enhancement.[25,35]

The supplementary material provides a numerical simulation of the group velocity for a periodically loaded transmission line.

DATA AVAILABILITY

The data that support the findings of this study are available from the corresponding author upon reasonable request.

REFERENCES

[1] F. Marsili, V. B. Verma, J. A. Stern, S. Harrington, A. E. Lita, T. Gerrits, I. Vayshenker, B. Baek, M. D. Shaw, R. P. Mirin et al., "Detecting single infrared photons with 93% system efficiency," Nat. Photonics **7**, 210–214 (2013).

[2] F. Marsili, F. Bellei, F. Najafi, A. E. Dane, E. A. Dauler, R. J. Molnar, and K. K. Berggren, "Efficient single photon detection from 500 nm to 5 μm wavelength," Nano Lett. **12**, 4799–4804 (2012).

[3] B. Korzh, Q.-Y. Zhao, J. P. Allmaras, S. Frasca, T. M. Autry, E. A. Bersin, A. D. Beyer, R. M. Briggs, B. Bumble, M. Colangelo et al., "Demonstration of sub-3 ps temporal resolution with a superconducting nanowire single-photon detector," Nat. Photonics **14**, 250–255 (2020).

[4] S. Ferrari, C. Schuck, and W. Pernice, "Waveguide-integrated superconducting nanowire single-photon detectors," Nanophotonics **7**, 1725–1758 (2018).

[5] S. Steinhauer, L. Yang, S. Gyger, T. Lettner, C. Errando-Herranz, K. D. Jöns, M. A. Baghban, K. Gallo, J. Zichi, and V. Zwiller, "NbTiN thin films for superconducting photon detectors on photonic and two-dimensional materials," Appl. Phys. Lett. **116**, 171101 (2020).

[6] R. Gourgues, J. W. N. Los, J. Zichi, J. Chang, N. Kalhor, G. Bulgarini, S. N. Dorenbos, V. Zwiller, and I. E. Zadeh, "Superconducting nanowire single photon detectors operating at temperature from 4 to 7 K," Opt. Express **27**, 24601–24609 (2019).

[7] I. Holzman and Y. Ivry, "Superconducting nanowires for single-photon detection: Progress, challenges, and opportunities," Adv. Quantum Technol. **2**, 1800058 (2019).

[8] A. W. Elshaari, W. Pernice, K. Srinivasan, O. Benson, and V. Zwiller, "Hybrid integrated quantum photonic circuits," Nat. Photonics **14**, 285–298 (2020).

[9] G. Gol'Tsman, O. Okunev, G. Chulkova, A. Lipatov, A. Semenov, K. Smirnov, B. Voronov, A. Dzardanov, C. Williams, and R. Sobolewski, "Picosecond superconducting single-photon optical detector," Appl. Phys. Lett. **79**, 705–707 (2001).

[10] A. Divochiy, F. Marsili, D. Bitauld, A. Gaggero, R. Leoni, F. Mattioli, A. Korneev, V. Seleznev, N. Kaurova, O. Minaeva et al., "Superconducting nanowire photon-number-resolving detector at telecommunication wavelengths," Nat. Photonics **2**, 302–306 (2008).

[11] D. Zhu, M. Colangelo, C. Chen, B. A. Korzh, F. N. C. Wong, M. D. Shaw, and K. K. Berggren, "Resolving photon numbers using a superconducting nanowire with impedance-matching taper," Nano Lett. **20**, 3858–3863 (2020).

[12] D. Zhu, M. Colangelo, B. A. Korzh, Q.-Y. Zhao, S. Frasca, A. E. Dane, A. E. Velasco, A. D. Beyer, J. P. Allmaras, E. Ramirez, W. J. Strickland, D. F. Santavicca, M. D. Shaw, and K. K. Berggren, "Superconducting nanowire single-photon detector with integrated impedance-matching taper," Appl. Phys. Lett. **114**, 042601 (2019).

[13] E. E. Wollman, V. B. Verma, A. E. Lita, W. H. Farr, M. D. Shaw, R. P. Mirin, and S. Woo Nam, "Kilopixel array of superconducting nanowire single-photon detectors," Opt. Express **27**, 35279–35289 (2019).

[14] I. Esmaeil Zadeh, J. W. N. Los, R. B. M. Gourgues, J. Chang, A. W. Elshaari, J. R. Zichi, Y. J. van Staaden, J. P. E. Swens, N. Kalhor, A. Guardiani, Y. Meng, K. Zou, S. Dobrovolskiy, A. W. Fognini, D. R. Schaart, D. Dalacu, P. J. Poole, M. E. Reimer, X. Hu, S. F. Pereira, V. Zwiller, and S. N. Dorenbos, "Efficient single-photon detection with 7.7 ps time resolution for photon-correlation measurements," ACS Photonics **7**, 1780–1787 (2020).

[15] S. Krinner, S. Storz, P. Kurpiers, P. Magnard, J. Heinsoo, R. Keller, J. Luetolf, C. Eichler, and A. Wallraff, "Engineering cryogenic setups for 100-qubit scale superconducting circuit systems," EPJ Quantum Technol. **6**, 2 (2019).

[16]S. Doerner, A. Kuzmin, S. Wuensch, I. Charaev, F. Boes, T. Zwick, and M. Siegel, "Frequency-multiplexed bias and readout of a 16-pixel superconducting nanowire single-photon detector array," Appl. Phys. Lett. **111**, 032603 (2017).

[17]A. Gaggero, F. Martini, F. Mattioli, F. Chiarello, R. Cernansky, A. Politi, and R. Leoni, "Amplitude-multiplexed readout of single photon detectors based on superconducting nanowires," Optica **6**, 823–828 (2019).

[18]J. Tiedau, T. Schapeler, V. Anant, H. Fedder, C. Silberhorn, and T. J. Bartley, "Single-channel electronic readout of a multipixel superconducting nanowire single photon detector," Opt. Express **28**, 5528–5537 (2020).

[19]R. Cheng, C.-L. Zou, X. Guo, S. Wang, X. Han, and H. X. Tang, "Broadband on-chip single-photon spectrometer," Nat. Commun. **10**, 4104 (2019).

[20]M. Hofherr, M. Arndt, K. Il'in, D. Henrich, M. Siegel, J. Toussaint, T. May, and H. Meyer, "Time-tagged multiplexing of serially biased superconducting nanowire single-photon detectors," IEEE Trans. Appl. Supercond. **23**, 2501205 (2013).

[21]Q.-Y. Zhao, D. Zhu, N. Calandri, A. E. Dane, A. N. McCaughan, F. Bellei, H.-Z. Wang, D. F. Santavicca, and K. K. Berggren, "Single-photon imager based on a superconducting nanowire delay line," Nat. Photonics **11**, 247 (2017).

[22]D. Zhu, Q.-Y. Zhao, H. Choi, T.-J. Lu, A. E. Dane, D. Englund, and K. K. Berggren, "A scalable multi-photon coincidence detector based on superconducting nanowires," Nat. Nanotechnol. **13**, 596–601 (2018).

[23]T. Berger and D. Tufts, "Optimum pulse amplitude modulation—I: Transmitter-receiver design and bounds from information theory," IEEE Trans. Inf. Theory **13**, 196–208 (1967).

[24]Y. A. Vlasov, M. O'Boyle, H. F. Hamann, and S. J. McNab, "Active control of slow light on a chip with photonic crystal waveguides," Nature **438**, 65–69 (2005).

[25]M. Mirhosseini, E. Kim, V. S. Ferreira, M. Kalaee, A. Sipahigil, A. J. Keller, and O. Painter, "Superconducting metamaterials for waveguide quantum electrodynamics," Nat. Commun. **9**, 3706 (2018).

[26]M. Göppl, A. Fragner, M. Baur, R. Bianchetti, S. Filipp, J. M. Fink, P. J. Leek, G. Puebla, L. Steffen, and A. Wallraff, "Coplanar waveguide resonators for circuit quantum electrodynamics," J. Appl. Phys. **104**, 113904 (2008).

[27]J. Rautio, "Electromagnetic analysis for microwave applications," in *Computational Electromagnetics and Its Applications* (Kluwer Academic Publishers, 2012), Vol. 5, pp. 80–96.

[28]N. Samkharadze, A. Bruno, P. Scarlino, G. Zheng, D. P. DiVincenzo, L. DiCarlo, and L. M. K. Vandersypen, "High-kinetic-inductance superconducting nanowire resonators for circuit QED in a magnetic field," Phys. Rev. Appl. **5**, 044004 (2016).

[29]J. Zichi, J. Chang, S. Steinhauer, K. von Fieandt, J. W. N. Los, G. Visser, N. Kalhor, T. Lettner, A. W. Elshaari, I. E. Zadeh, and V. Zwiller, "Optimizing the stoichiometry of ultrathin NbTiN films for high-performance superconducting nanowire single-photon detectors," Opt. Express **27**, 26579–26587 (2019).

[30]R. Gourgues, I. E. Zadeh, A. W. Elshaari, G. Bulgarini, J. W. N. Los, J. Zichi, D. Dalacu, P. J. Poole, S. N. Dorenbos, and V. Zwiller, "Controlled integration of selected detectors and emitters in photonic integrated circuits," Opt. Express **27**, 3710–3716 (2019).

[31]E. Le Coarer, S. Blaize, P. Benech, I. Stefanon, A. Morand, G. Lérondel, G. Leblond, P. Kern, J. M. Fedeli, and P. Royer, "Wavelength-scale stationary-wave integrated Fourier-transform spectrometry," Nat. Photonics **1**, 473–478 (2007).

[32]D. Pohl, M. Reig Escalé, M. Madi, F. Kaufmann, P. Brotzer, A. Sergeyev, B. Guldimann, P. Giaccari, E. Alberti, U. Meier *et al.*, "An integrated broadband spectrometer on thin-film lithium niobate," Nat. Photonics **14**, 24–29 (2020).

[33]A. J. Kerman, E. A. Dauler, W. E. Keicher, J. K. W. Yang, K. K. Berggren, G. Gol'tsman, and B. Voronov, "Kinetic-inductance-limited reset time of superconducting nanowire photon counters," Appl. Phys. Lett. **88**, 111116 (2006).

[34]W. H. P. Pernice, C. Schuck, O. Minaeva, M. Li, G. N. Goltsman, A. V. Sergienko, and H. X. Tang, "High-speed and high-efficiency travelling wave single-photon detectors embedded in nanophotonic circuits," Nat. Commun. **3**, 1325 (2012).

[35]A. Lai, C. Caloz, and T. Itoh, "Composite right/left-handed transmission line metamaterials," IEEE Microw. Mag. **5**, 34–50 (2004).